Available online at www.sciencedirect.com
ScienceDirect
Journal of Organometallic Chemistry 692 (2007) 4467–4472
Journal of Organometallic Chemistry
www.elsevier.com/locate/jorganchem

High-nuclearity ruthenium carbonyl cluster chemistry. 8: Phosphine activation, CO insertion, and deruthenation at a phosphido cluster – X-ray structures of $[ppn][Ru_8(\mu_8\text{-}P)(\mu\text{-}CO)_2(CO)_{20}]$ and $[ppn][Ru_7(\mu_7\text{-}P)(\mu\text{-}\eta^2\text{-}OCPh)(\mu\text{-}PPh_2)(\mu\text{-}CO)(CO)_{17}]$

Michael D. Randles [a], Anthony C. Willis [b], Marie P. Cifuentes [a], Mark G. Humphrey [a,*]

[a] Department of Chemistry, Australian National University, Canberra, ACT 0200, Australia
[b] Research School of Chemistry, Australian National University, Canberra, ACT 0200, Australia

Received 18 January 2007; received in revised form 26 March 2007; accepted 27 March 2007
Available online 2 April 2007

Dedicated to Professor Dr. Gerhard Erker, an inspirational organometallic chemist, on the occasion of his 60th birthday.

Abstract

Reaction of the square antiprismatic cluster $[ppn][Ru_8(\mu_8\text{-}P)(\mu\text{-}CO)_2(CO)_{20}]$ [ppn = bis(triphenylphosphoranylidene)ammonium] with triphenylphosphine proceeds by loss of one cluster core vertex, phosphine P–C cleavage, and CO insertion into the putative Ru–phenyl bond to afford $[ppn][Ru_7(\mu_7\text{-}P)(\mu\text{-}\eta^2\text{-}OCPh)(\mu\text{-}PPh_2)(\mu\text{-}CO)(CO)_{17}]$ in low yield, the first heptaruthenium μ_7-phosphido-ligated cluster.

Keywords: Crystal structure; Ruthenium; Phosphido; Interstitial; Cluster

1. Introduction

Low- and medium-nuclearity cluster chemistry is very well developed, but the chemistry of high-nuclearity clusters (M_n, $n \geqslant 7$) continues to be significantly less explored, largely a result of the dearth of facile routes into such species [1,2]. Where high-nuclearity clusters have been synthesized, they often show unusual and unanticipated reactivity and/or properties – we have previously reported the synthesis, ligand substitution chemistry, and a variety of physical properties studies of hydridodecaruthenium carbido clusters [3–8], for which striking differences in behavior to that of the corresponding osmium system were noted. More recently, we reported the synthesis and two structural modifications of $[ppn][Ru_8(\mu_8\text{-}P)(\mu\text{-}CO)_2(CO)_{20}]$ [9,10]. We report herein a third distinct crystal morphology of this cluster salt, together with its reactivity towards triphenylphosphine, and a structural study of the heptaruthenium cluster anion product as its bis(triphenylphosphine)iminium ($[ppn]^+$) salt.

2. Experimental

2.1. General conditions

All solvents and reagent triphenylphosphine (Aldrich) were used as received. Petrol refers to a fraction of boiling range 60–80 °C. The literature procedure was used to synthesize $[ppn][Ru_8(\mu_8\text{-}P)(\mu\text{-}CO)_2(CO)_{20}]$ [9]. The reaction products were purified by thin-layer chromatography (TLC) on 20×20 cm glass plates coated with Merck GF_{254} silica gel (0.5 mm).

* Corresponding author. Tel.: +61 2 6125 2927; fax: +61 2 6125 0760.
E-mail address: Mark.Humphrey@anu.edu.au (M.G. Humphrey).

0022-328X/$ - see front matter © 2007 Elsevier B.V. All rights reserved.
doi:10.1016/j.jorganchem.2007.03.040

IR spectra were recorded on a Perkin–Elmer System 2000 FT-IR with CaF_2 solution cells as solutions in dichloromethane (AR grade); spectral frequencies are recorded in cm^{-1}. The ^1H and ^{31}P NMR spectra were recorded in d_6-acetone (Cambridge Isotope Laboratories) using a Varian Gemini-300 spectrometer at 300 MHz or 121 MHz and referenced to residual non-perdeuterated solvent at 2.05 ppm or external H_3PO_4 at 0.0 ppm, respectively. The electrospray (ES) mass spectrum was recorded on a Bruker Apex 4.7 T FTICR-MS. MS data are reported in the form: m/z (assignment, relative intensity).

2.2. Synthesis of [ppn][$Ru_7(\mu_7$-P)(μ-η^2-OCPh)(μ-PPh_2)(μ-CO)(CO)$_{17}$] (2)

Triphenylphosphine (10.0 mg, 38.1 μmol) was added to a Schlenk tube containing [ppn][$Ru_8(\mu_8$-P)(μ-CO)$_2$(CO)$_{20}$] (19.5 mg, 9.78 μmol) in acetone (7 mL) under nitrogen, and the resultant solution stirred at room temperature for 70 h, while monitoring the progress of the reaction by IR. The solvent was removed *in vacuo*, and the crude residue dissolved in the minimum amount of acetone and applied to preparative silica TLC plates. Elution with acetone:petrol (9:11) afforded four bands. The contents of the first band ($R_f = 0.76$, orange) were extracted with CH_2Cl_2 to afford what appeared to be a mixture of products, the major component of which was probably $Ru_3(CO)_{10}(PPh_3)_2$ (11.4 mg) by IR spectral comparison. The contents of the second band ($R_f = 0.62$, purple) were extracted with CH_2Cl_2 to afford a purple solid, identified as unreacted [ppn][$Ru_8(\mu_8$-P)(μ-CO)$_2$(CO)$_{20}$] (**1**) (4.7 mg, 2.36 μmol, 24%). Diffusion of heptane into a solution of **1** in $CHCl_3$ at 4 °C gave dark purple crystals. The contents of the third band ($R_f = 0.49$, brown) were extracted with CH_2Cl_2 to afford a purple solid, identified as [ppn][$Ru_7(\mu_7$-P)(μ-η^2-OCPh)(μ-PPh_2)(μ-CO)(CO)$_{17}$] (**2**) (3.9 mg, 1.88 μmol, 19%). Diffusion of butanol into a solution of **2** in CH_2Cl_2 at 4 °C gave dark brown crystals. IR (CH_2Cl_2): ν(CO, cluster) 2064 m, 2029 vs, 2017 vs, 1995 m, 1973 w cm^{-1}. ^1H NMR (d_6-acetone): δ 7.74–7.50 (m, Ph). ^{31}P NMR (d^6-acetone): 600.3 (μ_8-P), 167.9 (PPh_2), 22.7 (ppn). MS (ESI): 1533 ([M]$^-$, 100). Insufficient material precluded microanalysis. The contents of the fourth band ($R_f = 0.36$, yellow) appeared to be in trace amounts and were not isolated.

2.3. X-ray structural studies of [ppn][$Ru_8(\mu_8$-P)(μ-CO)$_2$(CO)$_{20}$] (1) and [ppn][$Ru_7(\mu_7$-P)(μ-η^2-OCPh)(μ-PPh_2)(μ-CO)(CO)$_{17}$] (2)

The crystal and refinement data for compounds **1** and **2** are summarized in Table 1. Crystals suitable for the X-ray structural analyses were grown by liquid diffusion of heptane into a $CHCl_3$ solution (**1**) or liquid diffusion of 1-butanol into a dichloromethane solution (**2**) at 277 K. A single crystal of each species was mounted on a fine glass capillary, and data collected on a Nonius Kappa CCD diffractometer at 200 K using graphite monochromated Mo Kα radiation ($\lambda = 0.71073$ Å). The unit cell parameters were obtained by least-squares refinement [11] of 139 362 (**1**) or 153 941 (**2**) reflections with $3 \leqslant \theta \leqslant 25°$ (**1**) or $3 \leqslant \theta \leqslant 27°$ (**2**). The reduced data [11] were corrected for absorption using numerical methods [12] implemented from within MAXUS [13]; equivalent reflections were merged. The structures were solved by direct methods and refined with the use of the CRYSTALS software package [14].

Table 1
Crystal data and structure refinement details for [ppn][$Ru_8(\mu_8$-P)(μ-CO)$_2$(CO)$_{20}$] (**1**) and [ppn][$Ru_7(\mu_7$-P)(μ-η^2-OCPh)(μ-PPh_2)(μ-CO)(CO)$_{17}$] (**2**)

	1	**2**
Empirical formula	$C_{58}H_{30}NO_{22}P_3Ru_8$	$C_{75}H_{49}Cl_4NO_{19}P_4Ru_7$
Formula weight	1994.35	2241.41
Crystal size (mm)	$0.26 \times 0.04 \times 0.03$	$0.42 \times 0.37 \times 0.05$
Colour, habit	Purple, needle	Black, plate
Crystal system	Monoclinic	Monoclinic
Space group	$C2/c$	$P2_1/c$
a (Å)	12.4638(5)	19.6600(2)
b (Å)	31.084(1)	22.7838(2)
c (Å)	17.9687(6)	20.1337(1)
β (°)	94.619(2)	116.2726(4)
V (Å^3)	6938.9(4)	8086.9(1)
Z	4	4
D_{calc} (g cm^{-3})	1.909	1.841
μ (mm^{-1})	1.831	1.551
θ_{max} (°)	25.0	27.5
$N_{collected}$	139 362	167 487
N_{unique}	6115	18 503
$N_{observed}$	3070 ($I > 3.00\sigma(I)$)	12 087 ($I > 3.00\sigma(I)$)
Absorption correction	Integration	Integration
T_{min}, T_{max}	0.76, 0.96	0.49, 0.93
Number of parameters	418	981
R[a]	0.0320	0.0393
R_w[b]	0.0344	0.0467
S	1.15	1.09
$(\Delta/\rho)_{min}$ (e Å^{-3})	−0.52	−2.06
$(\Delta/\rho)_{max}$ (e Å^{-3})	1.48	1.86

[a] $R = \sum\|\|F_0| - |F_c\|| / \sum|F_0|$.
[b] $R_w = [(\sum w(|F_0| - |F_c|)^2 / \sum wF_0^2)]^{1/2}$.

The crystallographic asymmetric unit of **1** contains one half a ppn cation and one half a cluster anion, the other halves being generated by twofold rotation axes that pass through the cation N atom and anion interstitial phosphido ligand. The crystallographic asymmetric unit of **2** contains one ppn cation, one cluster anion, and two dichloromethane molecules of solvation. All non-hydrogen atoms of the ppn cation and cluster anion in **1** and **2** were refined with anisotropic displacement parameters. The dichloromethane molecules in **2** were found to be disordered over two sites each for which site occupancies were refined; the non-hydrogen atoms were refined isotropically. H atoms attached to C atoms were included in idealized positions and ride on the atoms to which they are bonded. The final cycles of matrix least-squares refinement were based on 3070 reflections and converged to $R = 0.032$ and $R_w = 0.035$ (**1**) or 12 087 reflections, converging to

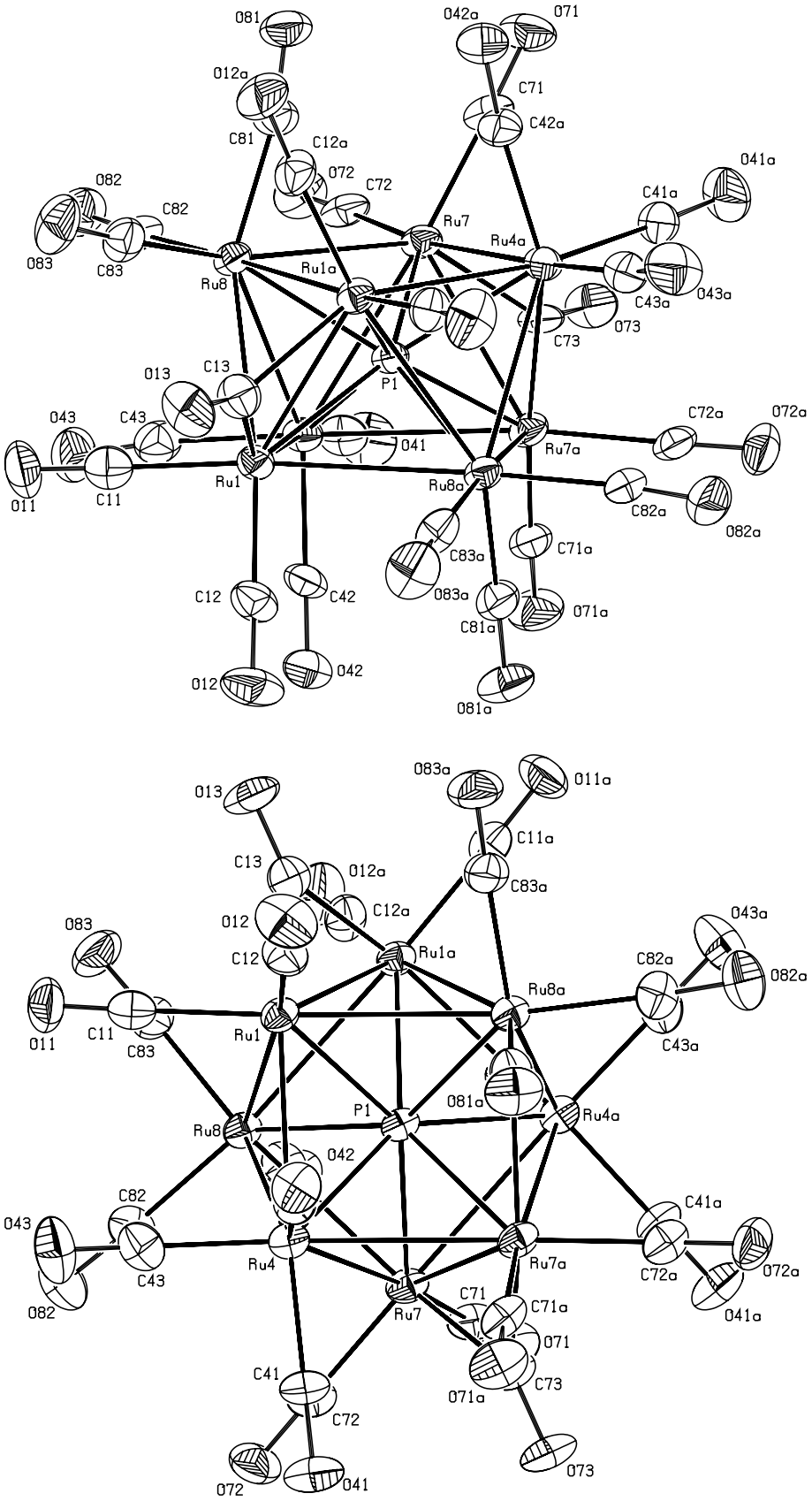

Fig. 1. ORTEP plots and atomic numbering scheme for the anion of [ppn][$Ru_8(\mu_8\text{-}P)(\mu\text{-}CO)_2(CO)_{20}$] (**1**). Displacement ellipsoids are at the 30% probability level.

Table 2
Selected bond lengths (Å) for [ppn][$Ru_8(\mu_8\text{-}P)(\mu\text{-}CO)_2(CO)_{20}$] (**1**)

Ru–Ru			
Ru(1)–Ru(2)	2.9725(8)	Ru(3)–Ru(6)	2.9127(7)
Ru(1)–Ru(4)	2.9108(8)	Ru(3)–Ru(7)	2.828(1)
Ru(1)–Ru(5)	2.797(1)	Ru(4)–Ru(7)	2.9127(7)
Ru(1)–Ru(8)	2.9026(7)	Ru(4)–Ru(8)	2.9202(7)
Ru(2)–Ru(3)	2.9191(8)	Ru(5)–Ru(6)	2.9108(8)
Ru(2)–Ru(5)	2.9026(7)	Ru(5)–Ru(8)	2.9725(8)
Ru(2)–Ru(6)	2.9202(7)	Ru(6)–Ru(7)	2.9510(8)
Ru(3)–Ru(4)	2.9510(8)	Ru(7)–Ru(8)	2.9191(8)
Ru–interstitial P			
Ru(1)–P	2.398(2)	Ru(5)–P	2.398(2)
Ru(2)–P	2.4049(9)	Ru(6)–P	2.3901(9)
Ru(3)–P	2.411(2)	Ru(7)–P	2.411(2)
Ru(4)–P	2.3901(9)	Ru(8)–P	2.4049(9)
Ru–bridging CO			
Ru(1)–C(13)	2.080(9)	Ru(3)–C(33)	2.080(7)
Ru(5)–C(13)	2.080(9)	Ru(7)–C(33)	2.080(7)

$R = 0.039$ and $R_w = 0.047$ (**2**). The largest peaks in the final difference electron map are located near the Ru (**1**) or Cl (**2**) atoms.

3. Results and discussion

3.1. X-ray structural study of [ppn][$Ru_8(\mu_8\text{-}P)(\mu\text{-}CO)_2(CO)_{20}$] (*1*)

We have previously reported two structural studies of the octaruthenium cluster anion starting material [9,10], and the present study has afforded a third distinct crystal polymorph. An ORTEP diagram of **1** is shown in Fig. 1, while selected cell data and crystallographic structure acquisition and processing parameters are collected in Table 1, and selected bond lengths are listed in Table 2. The structural study shows the square antiprismatic octaruthenium core and one interstitial phosphorus atom, and confirms that the carbonyl ligand disposition observed with the earlier studies (two edge-bridging carbonyl ligands, 20 terminal carbonyl ligands) is unchanged. The cluster has $8 \times 8(\text{Ru}) + 5(\text{P}) + 2 \times 2(\mu\text{-CO}) + 20 \times 2(\text{CO}) + 1(\text{charge}) = 114$ CVE. Its electron count is not consistent with the effective atomic number (EAN) rule, which predicts $8 \times 18(\text{metal atoms}) - 16 \times 2(\text{M} - \text{M}) = 112$ electrons, or Wade's rules (polyhedral skeletal electron-pair theory), for which an *arachno* bicapped square antiprism is predicted to have $14 \times 8(\text{metal atoms}) + 6 = 118$ electrons (seen, for example, in the square antiprismatic $[Ni_8(\mu_8\text{-}C)(\mu\text{-}CO)_8(CO)_8]^{2-}$ [15]), but is consistent with Lauher's cluster valence molecular orbital (CVMO) analysis, which predicts 57 CVMOs [16]; a 114 CVE count has been reported previously for $[Co_8(\mu_8\text{-}C)(\mu\text{-}CO)_9(CO)_9]^{2-}$ [17] and $Ru_8(\mu_8\text{-}P)(\mu\text{-}\eta^1\text{:}\eta^6\text{-}CH_2Ph)(\mu\text{-}CO)_2(CO)_{17}$ [18].

Although the core geometry and ligand disposition is maintained in these three studies, the majority of Ru–Ru bond lengths differ by >3 e.s.d. Differences are also apparent in Ru–P distances. In the two previous studies, the shorter Ru–P vectors are those to Ru2,4,6,8, whereas in the present structural determination, the shorter distances are those to Ru1,4,5,6, consistent with slightly different distortions from the idealized square antiprismatic hole. Both Ru–Ru and Ru–P distances are, on average, 0.006 Å shorter in the current study.

3.2. Synthesis of [ppn][$Ru_7(\mu_7\text{-}P)(\mu\text{-}\eta^2\text{-}OCPh)(\mu\text{-}PPh_2)(\mu\text{-}CO)(CO)_{17}$] (*2*)

Reaction between [ppn][$Ru_8(\mu_8\text{-}P)(\mu\text{-}CO)_2(CO)_{20}$] (**1**) and triphenylphosphine afforded the heptaruthenium cluster anion $[Ru_7(\mu_7\text{-}P)(\mu\text{-}\eta^2\text{-}OCPh)(\mu\text{-}PPh_2)(\mu\text{-}CO)(CO)_{17}]^-$ as its $[ppn]^+$ salt **2** in low yield (19%) (Scheme 1); its identity was established by IR, ^1H and ^{31}P NMR spectroscopy, electrospray mass spectrometry, and a single-crystal X-ray diffraction study. The solution IR spectrum shows the presence of terminal carbonyl ligands only, while the mass spectrum contains a molecular ion. The ^{31}P NMR spectrum contains a singlet at 600.3 ppm corresponding to the interstitial phosphorus, together with a singlet at 167.9 ppm due to the bridging phosphido, and a singlet at 22.7 ppm corresponding to the cation; the interstitial phosphorus resonance is slightly upfield of those of the precursor (620.4 and 774.8 ppm: see Ref. [9]). An ORTEP diagram from the structural study is shown in Fig. 2, while

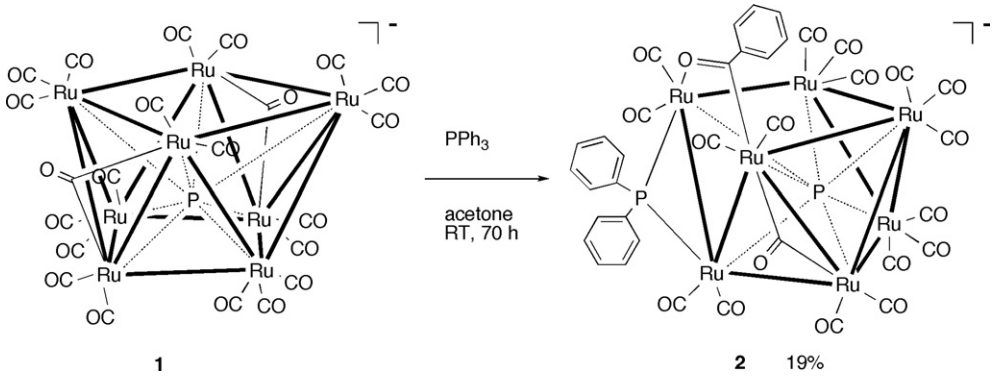

Scheme 1. Synthesis of **2**.

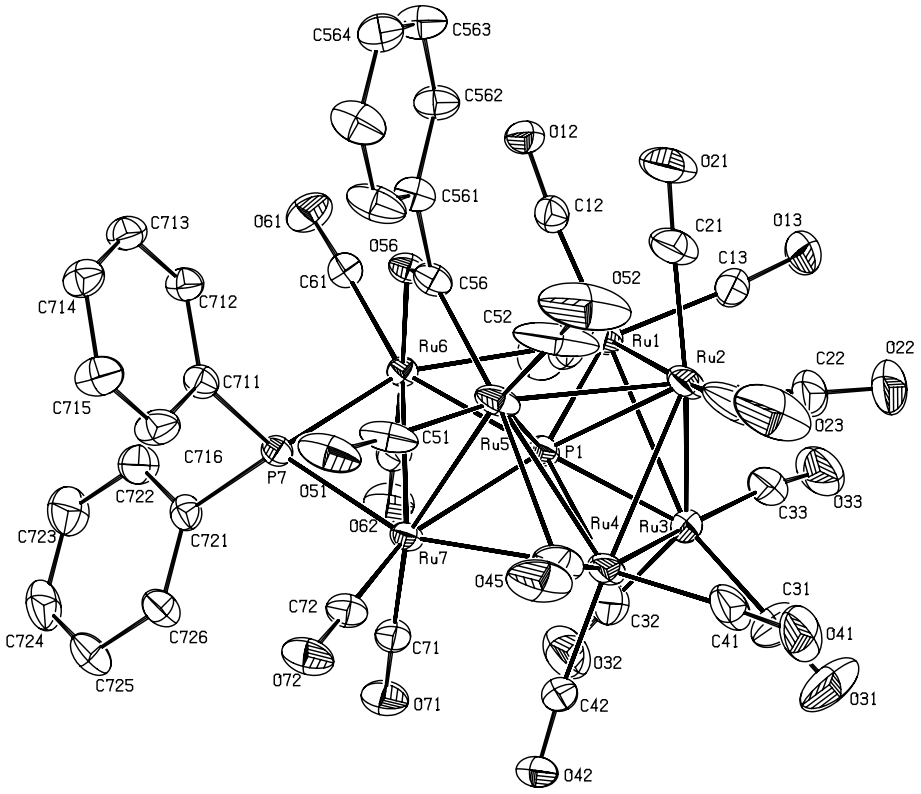

Fig. 2. ORTEP plots and atomic numbering scheme for the anion of [ppn][$Ru_7(\mu_7\text{-P})(\mu\text{-}\eta^2\text{-OCPh})(\mu\text{-PPh}_2)(\mu\text{-CO})(CO)_{17}$] (**2**). Displacement ellipsoids are at the 30% probability level.

important cell data and structure solution and refinement parameters are listed in Table 1, and selected bond lengths given in Table 3.

The structural study reveals an open heptaruthenium core with a phosphorus atom in bonding distance to all core metal atoms, a diphenylphosphido ligand bridging a Ru–Ru bond, a *C,O*-bound benzoyl ligand spanning a non-bonding Ru–Ru vector, seventeen terminal carbonyls, and one carbonyl bridging a Ru–Ru bond. The last-mentioned is formally semi-bridging (Curtis asymmetry parameter [19] $\alpha = 0.36$). The cluster possesses $7 \times 8(Ru) + 5(P) + 3(PhCO) + 3(PPh_2) + 2(\mu\text{-CO}) + 17 \times 2(CO) = 104$ CVE, which is EAN precise for an M_7 cluster with 11 M–M bonds.

Table 3
Selected bond lengths (Å) for [ppn][$Ru_7(\mu_7\text{-P})(\mu\text{-}\eta^2\text{-OCPh})(\mu\text{-PPh}_2)(\mu\text{-CO})(CO)_{17}$] (**2**)

Ru–Ru			
Ru1–Ru2	2.8860(6)	Ru1–Ru3	2.8862(5)
Ru1–Ru6	2.9288(5)	Ru2–Ru3	2.8431(7)
Ru2–Ru4	2.8740(5)	Ru2–Ru5	2.9459(7)
Ru3–Ru4	2.8768(7)	Ru4–Ru5	2.8878(6)
Ru4–Ru7	2.9485(5)	Ru5–Ru7	2.8115(5)
Ru6–Ru7	2.8661(4)		
Ru–interstitial P			
Ru1–P1	2.398(1)	Ru2–P1	2.414(1)
Ru3–P1	2.464(1)	Ru4–P1	2.435(1)
Ru5–P1	2.521(1)	Ru6–P1	2.477(1)
Ru7–P1	2.340(1)		
Ru–bridging ligands			
Ru6–P7	2.296(1)	Ru7–P7	2.271(1)
Ru4–C45	1.934(8)	Ru5–C45	2.623(5)
Ru5–C56	1.995(5)	Ru6–O56	2.159(3)
C56–O56	1.259(5)		

3.3. Discussion

Conversion of **1** into **2** involves expulsion of "$Ru(CO)_3$". IR analysis of a band obtained from TLC was suggestive of the presence of $Ru_3(CO)_{10}(PPh_3)_2$, a possible by-product considering that an excess of triphenylphosphine was employed. The core geometry of **2** is recognizable as possibly derived from that of **1** by excision of one ruthenium atom, together with cleavage of the Ru–Ru bond spanned by the benzoyl group (Scheme 2). The benzoyl and diphenylphosphido ligands probably arise from cluster-promoted activation of triphenylphosphine (almost certainly via a monodentate-PPh_3-ligated cluster) to give PPh_2 and Ph ligands, and insertion of CO into the putative Ru–C(phenyl) bond of the latter. The low yields of the product render any further speculation unwarranted.

Few heptaruthenium clusters are extant [1,2]; this is the first containing an atom with the maximum metal loading, although many examples with μ_6-C and one example each with μ_6-P [20] and μ_6-H [21] have been crystallographically confirmed.

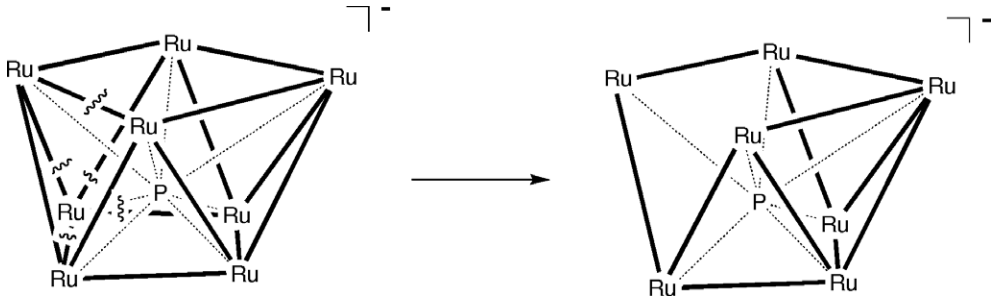

Scheme 2. Cluster core transformation in this study.

Acknowledgements

We thank the Australian Research Council (ARC) for support of this work and Johnson-Matthey Technology Centre for the generous loan of ruthenium salts. M.G.H. is an ARC Australian Professorial Fellow.

Appendix A. Supplementary material

CCDC 632596 and 632597 contain the supplementary crystallographic data for **1** and **2**. These data can be obtained free of charge via http://www.ccdc.cam.ac.uk/conts/retrieving.html, or from the Cambridge Crystallographic Data Centre, 12 Union Road, Cambridge CB2 1EZ, UK; fax: (+44) 1223-336-033; or e-mail: deposit@ccdc.cam.ac.uk. Supplementary data associated with this article can be found, in the online version, at doi:10.1016/j.jorganchem.2007.03.040.

References

[1] M.P. Cifuentes, M.G. Humphrey, in: E.W. Abel, F.G.A. Stone, G. Wilkinson (Eds.), Comprehensive Organometallic Chemistry II, vol. 7, Elsevier, Oxford, 1995, p. 909.
[2] M.G. Humphrey, M.P. Cifuentes, in: R. Crabtree, D.M.P. Mingos (Eds.), Comprehensive Organometallic Chemistry III, vol. 6, Elsevier, Oxford, 2006, p. 973.
[3] M.P. Cifuentes, M.G. Humphrey, B.W. Skelton, A.H. White, Organometallics 12 (1993) 4272.
[4] M.P. Cifuentes, M.G. Humphrey, B.W. Skelton, A.H. White, Organometallics 14 (1995) 1536.
[5] M.P. Cifuentes, M.G. Humphrey, B.W. Skelton, A.H. White, J. Organomet. Chem. 507 (1996) 163.
[6] M.P. Cifuentes, M.G. Humphrey, A.C. Willis, J. Organomet. Chem. 513 (1996) 85.
[7] M.P. Cifuentes, M.G. Humphrey, J.E. McGrady, P.J. Smith, R. Stranger, K.S. Murray, B. Moubaraki, J. Am. Chem. Soc. 119 (1997) 2647.
[8] M.P. Cifuentes, M.G. Humphrey, G.A. Heath, Inorg. Chim. Acta 259 (1997) 273.
[9] M.P. Cifuentes, S.M. Waterman, M.G. Humphrey, G.A. Heath, B.W. Skelton, A.H. White, M.P.S. Perera, M.L. Williams, J. Organomet. Chem. 565 (1998) 193.
[10] M.D. Randles, A.C. Willis, M.P. Cifuentes, M.G. Humphrey, Acta Crystallogr., Sect. E 62 (2006) m2350.
[11] Z. Otwinowski, W. Minor, in: C.W. Carter Jr., R.M. Sweet (Eds.), Methods in Enzymology, Academic Press, New York, 1997, p. 307.
[12] P. Coppens, in: F.R. Ahmed, S.R. Hall, C.P. Huber (Eds.), Crystallographic Computing, Munksgaard, Copenhagen, 1970, p. 255.
[13] S. Mackay, C.J. Gilmore, C. Edwards, N. Stewart, K. Shankland, MAXUS: Computer Program for the Solution and Refinement of Crystal Structures, Nonius, MacScience, and The University of Glasgow, The Netherlands, Japan, and UK, 1999.
[14] P.W. Betteridge, J.R. Carruthers, R.I. Cooper, C.K. Prout, D.J. Watkin, J. Appl. Crystallogr. 36 (2003) 1487.
[15] A. Ceriotti, G. Longoni, M. Manassero, M. Perego, M. Sansoni, Inorg. Chem. 24 (1985) 117.
[16] J.W. Lauher, J. Am. Chem. Soc. 100 (1978) 5305.
[17] V.G. Albano, P. Chini, G. Ciani, M. Sansoni, D. Strumolo, B.T. Heaton, S. Martinengo, J. Am. Chem. Soc. 98 (1976) 5027.
[18] L.M. Bullock, J.S. Field, R.J. Haines, E. Minshall, D.N. Smit, G.M. Sheldrick, J. Organomet. Chem. 310 (1986) C47.
[19] R.J. Klingler, W.M. Butler, M.D. Curtis, J. Am. Chem. Soc. 100 (1978) 5034.
[20] P. Frediani, M. Bianchi, A. Salvini, F. Piacenti, S. Ianelli, M. Nardelli, J. Chem. Soc., Dalton Trans (1990) 1705.
[21] R.D. Adams, J.E. Babin, J.T. Tanner, Organometallics 7 (1988) 2027.